JOURNAL OF MATERIALS SCIENCE 25 (1990) 1656–1661

Effects of microstructure on the R-curve behaviour of sintered silicon nitride

AKIRA OKADA, NAOTO HIROSAKI
Materials Research Laboratory, Central Engineering Laboratories, Nissan Motor Co., 1 Natsushima-cho, Yokosuka, Kanagawa 237, Japan

The R-curve behaviour of sintered silicon nitride was investigated by using short bar specimens. The samples were fabricated by sintering at 1700° C for 2 or 8 h in a nitrogen atmosphere, varying the initial α contents of the silicon nitride powder. The R-curve was evaluated with a loading and unloading technique to calculate K_R during stable fracture. Steep R-curves were observed in the specimens made from the high initial α content powder. Thus, the grain-bridging effect behind the crack seems to contribute to the R-curve, because a steep R-curve corresponds to fibrous texture development. Apparent K_C values with an assumption of linear elastic fracture mechanics for the specimens undergoing 8 h sintering, are greater than those undergoing 2 h sintering. These results can be attributed to microcracking.

1. Introduction

The fracture toughness of sintered silicon nitride along with oxide additives is known to be dependent on its grain morphology [1–4]. For instance, a higher fracture toughness is obtained by using a higher α-phase-content Si_3N_4 powder as a raw material in order to develop the fibrous microstructure during sintering [1–3]. This is because considerable work is required to pull out the fibrous Si_3N_4 grain from the matrix of the grain-boundary glassy phase [2, 5].

The fracture toughness also increases with increasing amount of additive oxides [4]. This can be attributed to the microcracking and the successive crack branching caused by the thermal expansion mismatch between the grain-boundary glassy phase and the Si_3N_4 grain. The R-curve behaviour of the sintered silicon nitride is affected by these toughening mechanisms.

This study was thus aimed at investigating the dependence of microstructure on the R-curve of sintered silicon nitride.

2. Compliance analysis with short bar specimens

Fig. 1 shows the configuration of a short bar specimen with a chevron notch which has been developed for K_{IC} measurement based on linear elastic fracture mechanics [6]. The short bar specimen has the advantage of stable fracture being easily achieved, such that K_{IC} can be calculated from the maximum load with no need for crack length measurement.

Considering the R-curve effects of the fracture process, a procedure for calculating K_I during stable fracture is needed. The stress intensity factor, K_I, is given by [7]

$$K_I = P\left(\frac{dC}{d\alpha}\frac{E}{1-\nu^2}\Big/2Wb\right)^{1/2} \quad (1)$$

where C is the compliance of the short bar specimen, P is the load, E is Young's modulus, ν is Poisson's ratio, W is the length of the specimen, b is the crack front width, and $\alpha = a/W$ at the crack length, a.

The relationship between the crack length and the compliance was determined by Barker [8], who reported a relative gradient of the load–displacement curve, r, against a/B, where B is the specimen width. The relative gradient is expressed by

$$r = M/M_0 = C_0/C \quad (2)$$

where M_0 is the original gradient without crack extension, M is the gradient after crack growth, and C_0 is the original compliance.

Using the load output of a Terratek Fractometer testing machine, P_F, a maximum value of which is translated into K_{IC} assuming linear elastic fracture mechanics, the stress intensity factor, K_I, can be calculated by [9]

$$K_I = AP_F[d(r^{-1})/dS]^{1/2} \quad (3)$$

Here, A is a constant value of 3.71×10^{-3} m, and S is the area covered by the crack. This equation indicates that the stress intensity during stable fracture can be calculated from the load output, P_F, and the relative gradient, r, as a function of S.

3. Experimental procedure

3.1. Sample preparation

Alpha-phase-rich silicon nitride powder, SN9S (Denki Kagaku Kogyo, Tokyo, Japan), β-phase-rich powder, SNBS (Denki Kagaku Kogyo, Tokyo, Japan), yttria (Shinetsu Chemical, Tokyo, Japan, 99.9%, pure), and alumina (Alcoa A-SG16, Pittsburgh, USA) were used as the raw materials. The phase content of silicon nitride powder was determined by X-ray diffraction analysis [10]: SN9S powder contains 95% α-Si_3N_4 and 5% β-Si_3N_4; and SNBS powder contains 31% α-Si_3N_4 and 69% β-Si_3N_4. The Si_3N_4 powders were mixed

0022–2461/90 $03.00 + .12

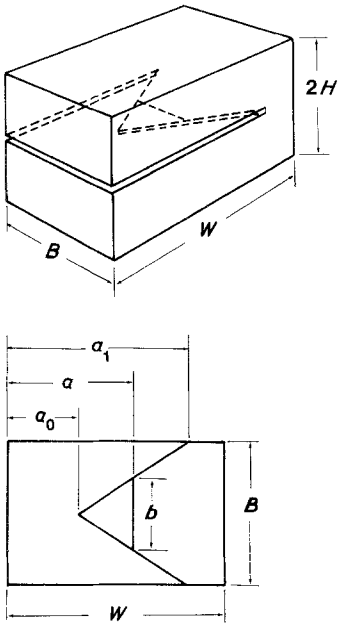

Figure 1 The configuration of a short bar specimen. The dimensions are: B = 12.70 mm, W = 19.05 mm, $2H$ = 11.05 mm, a_0 = 6.74 mm, and θ = 55.2°.

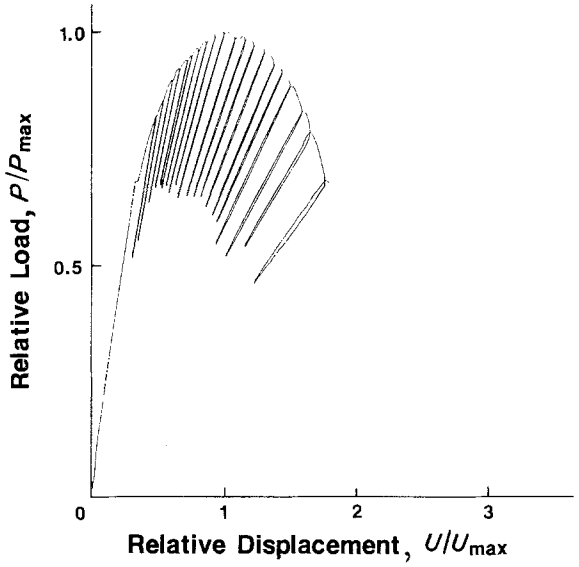

Figure 2 A typical load–displacement curve for a short bar specimen of sintered silicon nitride. Displacement at the maximum load (P_{max}) is denoted by U_{max}.

with 10% Y_2O_3 and 5% Al_2O_3 in a ball mill for 96 h. The initial α-phase content of silicon nitride powder was modified by varying the mixing ratio of the two powders. The dried powders were isostatically pressed at 196 MPa for sintering at 1700° C for 2 or 8 h in a nitrogen atmosphere.

Table I shows the densities of the sintered specimens. The densities of those specimens made from SN9S presented almost constant values of 3.31 g cm^{-3}, while the densities from the SNBS powder demonstrated a slight dependence on the sintering time: 3.15 g cm^{-3} for 2 h sintering and 3.28 g cm^{-3} for 8 h sintering. The phase detected by X-ray diffraction in the sintered specimen was β-Si_3N_4 for all cases.

The sintered specimens were ground to the dimensions 12.70 mm wide by 19.05 mm long by 11.05 mm thick. The chevron notches were introduced using a notch angle, θ, of 55.2° and a notch length, a_0, of 6.74 mm.

3.2. R-curve evaluation

A fractometer 4201 (Terratek Inc., Salt Lake City, UT) was used for evaluating the R-curve. The slot was opened by increasing the pressure of the mercury in a thin metal bag, called a flatjack, inserted in the chevron notch. The opening displacement was measured according to the thickness change in the specimen by the output voltage of the strain gauge attached to the specimen holder. During the stable fracture process, loading and unloading were repeated to obtain the relative gradient, r. The crack growth resistance, K_R, was calculated from the relative gradient and the load during stable fracture. The apparent critical stress intensity, K_C, which corresponds to the value calculated from the maximum load assuming linear elastic fracture mechanics, was read from the fractometer display.

4. Results

Fig. 2 shows a typical load–displacement curve. The load linearly increases with the opening of the chevron slot until pop-in occurs. When pop-in with a sudden load drop occurs, the initial crack is introduced at the tip of the slot. Stable crack propagation by further increasing the pressure of the mercury in the flatjack results in a decrease in the gradient of the load–displacement curve. As is clear, the load increased gradually to reach the maximum value, and then began to decrease.

Fig. 3 shows the apparent K_C values obtained. It is evident that the K_C value increases with increasing initial α content of the Si_3N_4 powder, and is higher for the 8 h sintering than for the 2 h sintering.

The results of the R-curve measurements are presented in Fig. 4. The K_R value increases with increasing crack length, and the slope of the R-curve is steeper when using the higher initial α-Si_3N_4 content powder. In particular, when the silicon nitride powder

TABLE I Apparent densities and phases of sintered silicon nitride with the additions of Y_2O_3 and Al_2O_3

Sample	Raw Si_3N_4 powder	Sintering condition	Density (g cm^{-3})	Phases
1	SNBS	1700° C, 2 h	3.31	β-Si_3N_4
2	SNBS/SN9S = 7/3	1700° C, 2 h	3.31	β-Si_3N_4
3	SNBS/SN9S = 3/7	1700° C, 2 h	3.29	β-Si_3N_4
4	SN9S	1700° C, 2 h	3.15	β-Si_3N_4
5	SNBS	1700° C, 8 h	3.31	β-Si_3N_4
6	SNBS/SN9S = 7/3	1700° C, 8 h	3.31	β-Si_3N_4
7	SNBS/SN9S = 3/7	1700° C, 8 h	3.31	β-Si_3N_4
8	SN9S	1700° C, 8 h	3.28	β-Si_3N_4

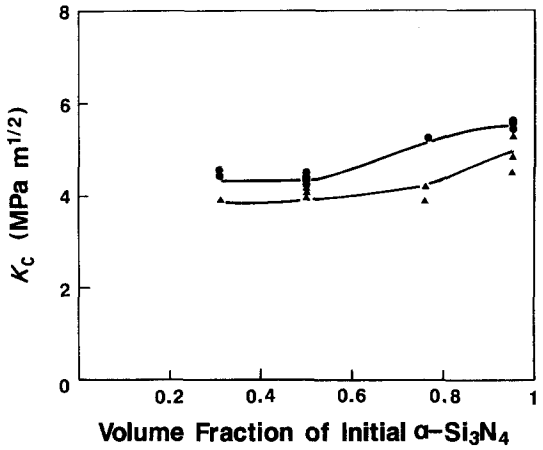

Figure 3 The K_C values for silicon nitride sintered at 1700° C for (●) 8 h, or (▲) 2 h, with addition of Y_2O_3 and Al_2O_3. The K_C values are obtained from the Fractometer display and plotted against the α phase content of the raw Si_3N_4 powder.

having an α content of 95% was employed as a raw material, a steep R-curve and high K_R values were obtained.

Scanning electron micrographs of the fracture surface are given in Fig. 5. The fracture surfaces of the sintered specimens having the higher α content Si_3N_4 powder show the developed fibrous texture pulled out from the matrix. In addition, the grain size of the specimens sintered for 8 h was greater than that sintered for 2 h.

5. Discussion

The sintered specimen produced from the high α content Si_3N_4 powder has a high K_C value and exhibits a tortuous fracture surface. This high K_C value should be attributed to the pull-out mechanism [5] or to the crack deflection mechanism [11]. The specimen sintered for 8 h has a coarser texture and a greater K_C value than that sintered for 2 h, while the aspect ratios of the Si_3N_4 grain and the apparent densities were almost the same.

The prolonged sintering results in grain growth rather than in elongated Si_3N_4 grains. This result is contrary to that found in the study conducted by Himsolt *et al.* [3], who reported that the fibrous grain developed when the hot-pressing time of Si_3N_4 was increased. This inconsistency can be attributed to the difference in the additive oxide for promoting sintering. Himsolt *et al.* employed magnesia, which promotes sintering rather than elongates the Si_3N_4 grain. However, the additions of yttria and alumina are known to develop the fibrous texture [12]. Thus, in the case of the yttria and alumina additions, the fibrous texture has been developed in an earlier stage of sintering than

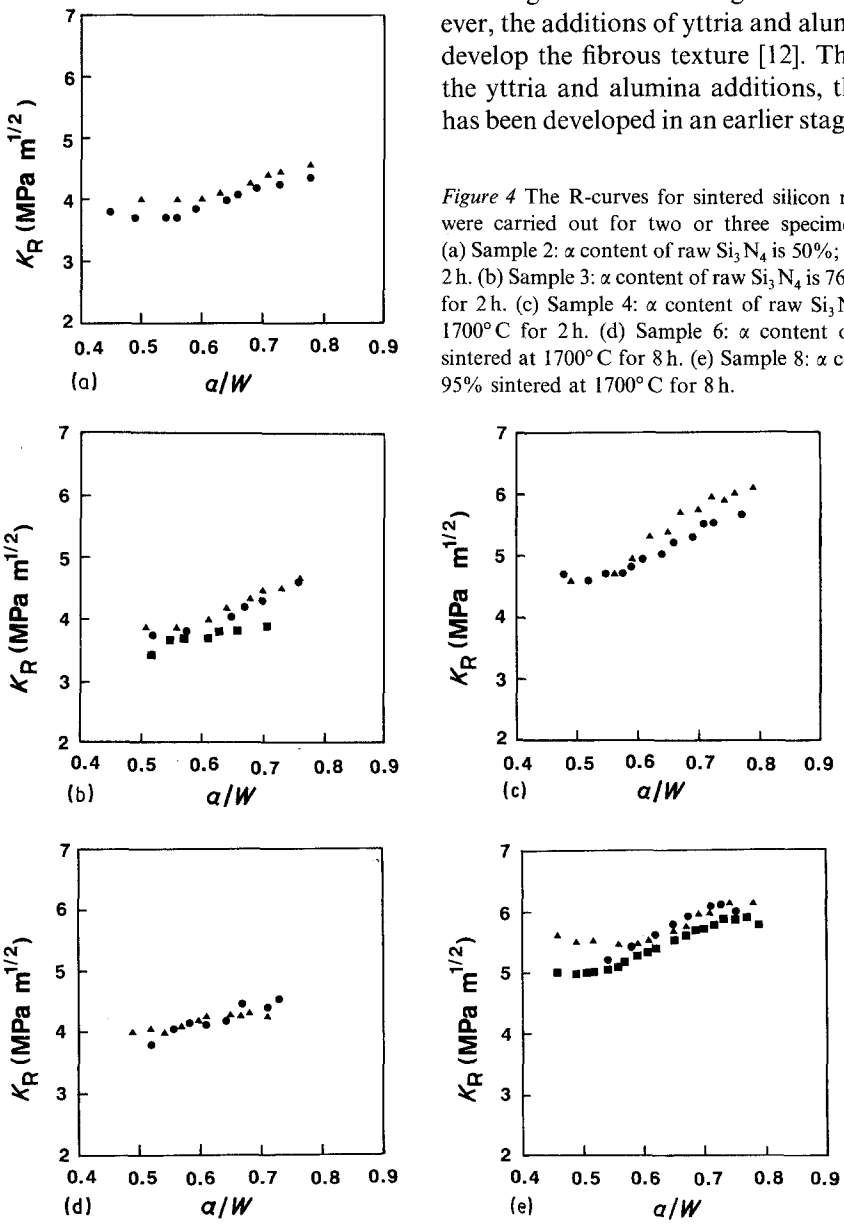

Figure 4 The R-curves for sintered silicon nitride. Measurements were carried out for two or three specimens of each material. (a) Sample 2: α content of raw Si_3N_4 is 50%; sintered at 1700° C for 2 h. (b) Sample 3: α content of raw Si_3N_4 is 76%; sintered at 1700° C for 2 h. (c) Sample 4: α content of raw Si_3N_4 is 95%; sintered at 1700° C for 2 h. (d) Sample 6: α content of raw Si_3N_4 is 50%; sintered at 1700° C for 8 h. (e) Sample 8: α content of raw Si_3N_4 is 95% sintered at 1700° C for 8 h.

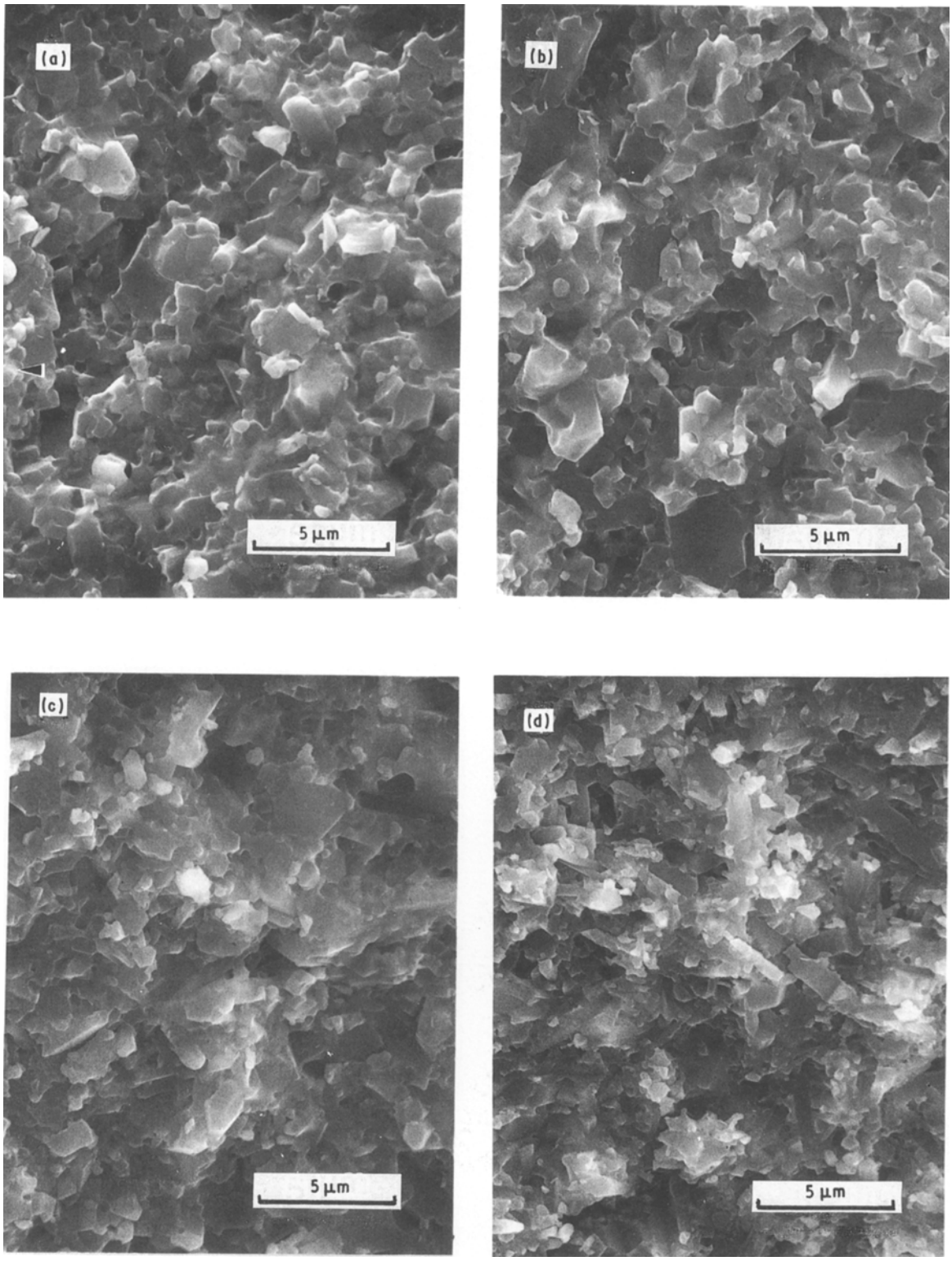

Figure 5 Scanning electron micrographs of the fracture surface of sintered silicon nitride. (a) Sample 1: α content of raw Si_3N_4 is 31%; sintered at 1700° C for 2 h. (b) Sample 2: α content of raw Si_3N_4 is 50%; sintered at 1700° C for 2 h. (c) Sample 3: α content of raw Si_3N_4 is 76%; sintered at 1700° C for 2 h. (d) Sample 4: α content of raw Si_3N_4 is 95%; sintered at 1700° C for 2 h. (e) Sample 5: α content of raw Si_3N_4 is 31%; sintered at 1700° C for 8 h. (f) Sample 6: α content of raw Si_3N_4 is 50%; sintered at 1700° C for 8 h. (g) Sample 7: α content of raw Si_3N_4 is 76%; sintered at 1700° C for 8 h. (h) Sample 8: α content of raw Si_3N_4 is 95%; sintered at 1700° C for 8 h.

that with a small amount of magnesia added. The higher K_C values for the 8 h sintering result from the grain growth. This is because the internal stress due to the thermal expansion mismatch between the Si_3N_4 grain and the grain-boundary glassy phase contributes to the microcracking in the region near the crack tip by causing the internal stress to interact with the stress field near the crack tip.

According to Green's calculation [13], the area causing the stress-induced microcracking in the system containing the spherical secondary phase extends more broadly when the size of the secondary phase is greater. Because the sintered Si_3N_4 has a secondary glass phase, the grain growth of Si_3N_4 also leads to the growth of the secondary phase resulting in an increasing microcracking zone to produce the higher K_C value.

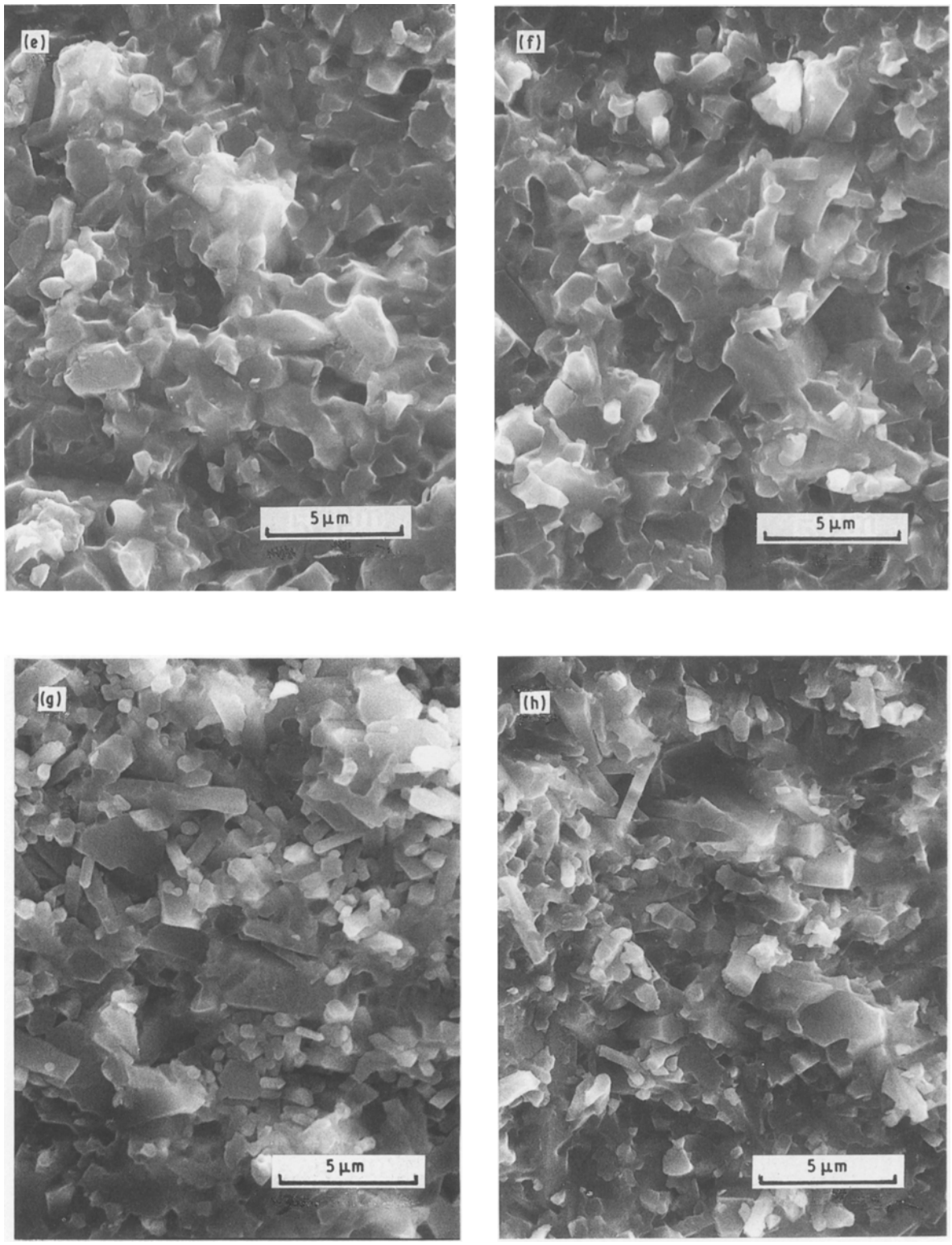

Figure 5 Continued

The steep slope of the R-curve should be observable in the initial stage of crack advance when the microcracking occurs in the area near the crack tip [14]. However, this initial increase in K_R was not detected in this study. This is because the pop-in introduces the initial crack advance about 1 mm, which conceals the initial stage of the steep R-curve caused by microcracking. The steep R-curve observed in the specimen from the high α-Si_3N_4 does not result from microcracking, but is rather caused by the fibrous grain development. The friction effect behind the crack seems to result in the steep R-curve [15, 16]. This is because the fibrous grain development produces a rough fracture surface, which can transfer the load through the contact points of the crack walls. Thus, the increased number of contact points accompanied with crack advance results in the rising R-curve.

6. Conclusions

The R-curve behaviour of sintered silicon nitride with the addition of yttria and alumina was evaluated using short bar specimens to investigate the effects of

its microstructure. The following conclusions were obtained.

1. Higher K_C values were obtained for sintered silicon nitride produced from the high α-phase content powder. The pull-out mechanism or the crack deflection mechanism is likely to be the major toughening mechanism in this case. Each mechanism can result from the fibrous grain development through the use of the higher α content Si_3N_4 powder.

2. The K_C value was higher with the 8 h sintering than that with the 2 h sintering. The prolonged sintering results in grain growth rather than in elongated grain development. The microcracking is likely to be the main contribution to this phenomenon.

3. The sintered silicon nitride with the fibrous microstructure has a steep R-curve slope, which seems to be caused by the grain-bridging effect behind the crack which lowers the crack-tip stress field.

References

1. F. F. LANGE, *J. Amer. Ceram. Soc.* **56** (1973) 518.
2. *Idem, ibid.* **62** (1979) 428.
3. G. HIMSOLT, H. KNOCH, H. HUEBNER and F. W. KLEINLEIN, *ibid.* **62** (1979) 29.
4. R. W. RICE, K. R. McKINNEY, C. C. WU, S. W FREIMAN and W. J. M. DONOUGH, *J. Mater. Sci.* **20** (1985) 1392.
5. F. F. LANGE, in "Fracture Mechanics of Ceramics", Vol. 4, edited by R. C. Bradt, D. P. H. Hasselman and F. F. Lange (Plenum, New York, 1978) p. 799.
6. L. M. BARKER, in "Fracture Mechanics of Ceramics", Vol. 3, edited by R. C. Bradt, D. P. H. Hasselman and F. F. Lange (Plenum, New York, 1978) p. 483.
7. D. MUNZ, R. T. BUBSEY and J. E. SRAWLEY, *Int. J. Fract.* **16** (1980) 359.
8. L. M. BARKER, *Engng Fract. Mech.* **17** (1983) 289.
9. A. OKADA and N. HIROSAKI and K. MATOBA, *Yogyo-Kyokai-shi* **95** (1987) 559.
10. C. P. GAZZARA and D. R. MESSIER, *Amer. Ceram. Soc. Bull.* **56** (1977) 777.
11. K. T. FABER and A. G. EVANS, *Acta. Metall.* **31** (1983) 565.
12. G. WOTTING and G. ZIEGLER, in "Ceramic Powders", edited by P. Vincenzini (Elsevier, Amsterdam, 1983) p. 951.
13. D. J. GREEN, *J. Amer. Ceram. Soc.* **64** (1981) 138.
14. A. G. EVANS and K. T. FABER, *ibid.* **67** (1984) 255.
15. A. BORNHAUSNER, K. KROMP and R. F. PABST, *J. Mater. Sci.* **20** (1985) 2586.
16. P. L. SWANSON, C. J. FAIRBANKS, B. R. LAWN, Y. W. MAI and B. J. HOCKEY, *J. Amer. Ceram. Soc.* **70** (1987) 276.

Received 12 December 1988
and accepted 23 August 1989